We are IntechOpen,
the world's leading publisher of
Open Access books
Built by scientists, for scientists

4,800
Open access books available

122,000
International authors and editors

135M
Downloads

Our authors are among the

154
Countries delivered to

TOP 1%
most cited scientists

12.2%
Contributors from top 500 universities

CLARIVATE ANALYTICS
BOOK
CITATION
INDEX
INDEXED

WEB OF SCIENCE™

Selection of our books indexed in the Book Citation Index
in Web of Science™ Core Collection (BKCI)

Interested in publishing with us?
Contact book.department@intechopen.com

Numbers displayed above are based on latest data collected.
For more information visit www.intechopen.com

Transition Metal Chalcogenides for the Electrocatalysis of Water

Chi-Ang Tseng and Chuan-Pei Lee

Abstract

Sustainable energy technology has received enormous attention in recent years. Specifically, electrochemical water splitting is considered to be the cleanest technique for the production of promising fuels, for example, hydrogen and oxygen, where transition metal (di)chalcogenides (TMCs) as electrocatalysts for hydrogen evolution reaction (HER) and oxygen evolution reaction (OER) have been a growing interest. In this chapter, the typical preparation methods of TMCs such as chemical vapor phase deposition (CVD) and solvothermal synthesis are introduced. Then, several TMC materials for catalyzing HER and OER are reviewed. Most importantly, this chapter also introduced some *in situ* approaches to realize the mechanism of electrocatalytic behavior toward HER and OER. Finally, the conclusion and futuristic prospects of TMCs in HER and OER are discussed.

Keywords: energy conversion, hydrogen evolution reaction (HER), oxygen evolution reaction (OER), transition metal chalcogenides (TMCs)

1. Introduction

Energy crisis and environmental pollution arising from the burning of carbon-based fossil fuel in the past decades facilitate people to reconsider the way we utilized the resource on earth. Hydrogen as an ideal energy source came up to the stage due to its high energy density and environmental benignity [1, 2]. Electrochemical water splitting is not only regarded as the cleanest technique for hydrogen generation but also suitable to perform on a large scale. The appropriate electrocatalysts are developed to boost the cathodic hydrogen evolution reaction (HER) and anodic oxygen evolution reaction (OER) because of the sluggish kinetics of these two core reactions [overpotential (η), **Figure 1a**]. Although platinum-based and iridium/ruthenium-based catalysts, respectively, have shown very promising performance in HER and OER, the industrial application is restricted due to their high cost and limited availability [3, 4]. Thus, developing alternative electrocatalysts based on non-noble metals or earth-abundant elements is still highly demanded.

The realization of HER and OER mechanisms plays a crucial role to design the efficient electrocatalysts, so the brief discussions on their mechanisms were introduced.

Two kinds of HER mechanisms have been completely studied and widely accepted [5, 6]. The first step, a proton from the solution adsorbs onto the catalytic sites of the electrode with a reduction process, is called as Volmer step:
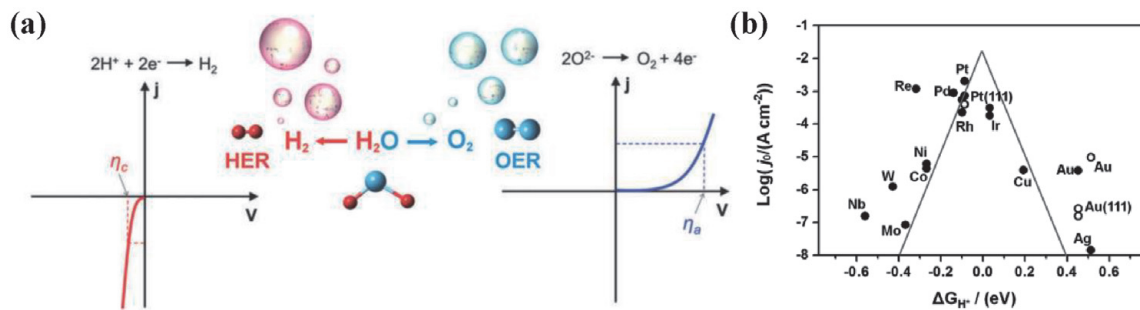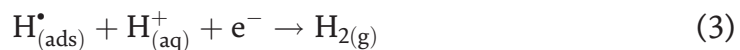
Figure 1.
(a) Polarization curves for HER and OER [9] and (b) volcano plot of exchange current density (j_o) as a function of DFT-calculated Gibbs free energy (ΔG_H) of adsorbed atomic hydrogen on pure metals [7].
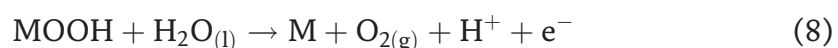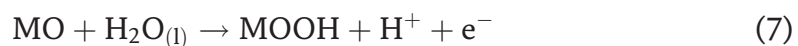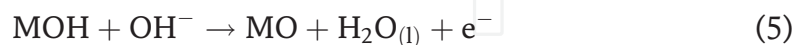
$$H^+_{(aq)} + e^- \rightarrow H^{\bullet}_{(ads)} \tag{1}$$

Then, either the recombination of two adsorbed hydrogen atoms on the electrode surface is called as Tafel step:

$$H^{\bullet}_{(ads)} + H^{\bullet}_{(ads)} \rightarrow H_{2(g)} \tag{2}$$

or the reaction of an adsorbed hydrogen atom with the hydrated proton, which proceeds with an electron transfer from the electrode surface, is called as Heyrovsky step:

$$H^{\bullet}_{(ads)} + H^+_{(aq)} + e^- \rightarrow H_{2(g)} \tag{3}$$

Nørskov et al. proposed a Volcano curve showing that experimental exchange currents of materials are as a function of the Gibbs free energy of the adsorbed hydrogen (ΔG_H) (**Figure 1b**) [7, 8]. Ideally, the interaction of hydrogen with the electrode surface should be thermoneutral ($\Delta G_H \cong 0$), otherwise either Heyrovsky or Tafel step (strong bonding) or Volmer step would become the rate-determining step. In the case of the OER, many researchers have proposed possible mechanisms at the anode in acidic electrolyte (Eqs. (4)–(8)). However, there are some differences around the reaction of forming oxygen. One route of forming oxygen is through the direct recombination of two MO (M represents Mn, Fe, Co, and Ni metals) (Eq. (6)), while the other route of forming oxygen is through the decomposition of the MOOH intermediate (Eq. (8)).

$$M + H_2O_{(l)} \rightarrow MOH + H^+ + e^- \tag{4}$$

$$MOH + OH^- \rightarrow MO + H_2O_{(l)} + e^- \tag{5}$$

$$2MO \rightarrow 2M5 + O_{2(g)} \tag{6}$$

$$MO + H_2O_{(l)} \rightarrow MOOH + H^+ + e^- \tag{7}$$

$$MOOH + H_2O_{(l)} \rightarrow M + O_{2(g)} + H^+ + e^- \tag{8}$$

2. Preparations of TMCs

2.1 CVD synthesis of TMCs

The preparation methods of TMCs layers can be categorized into two main approaches: top-down and bottom-up methods (**Figure 2**). The TMC layers
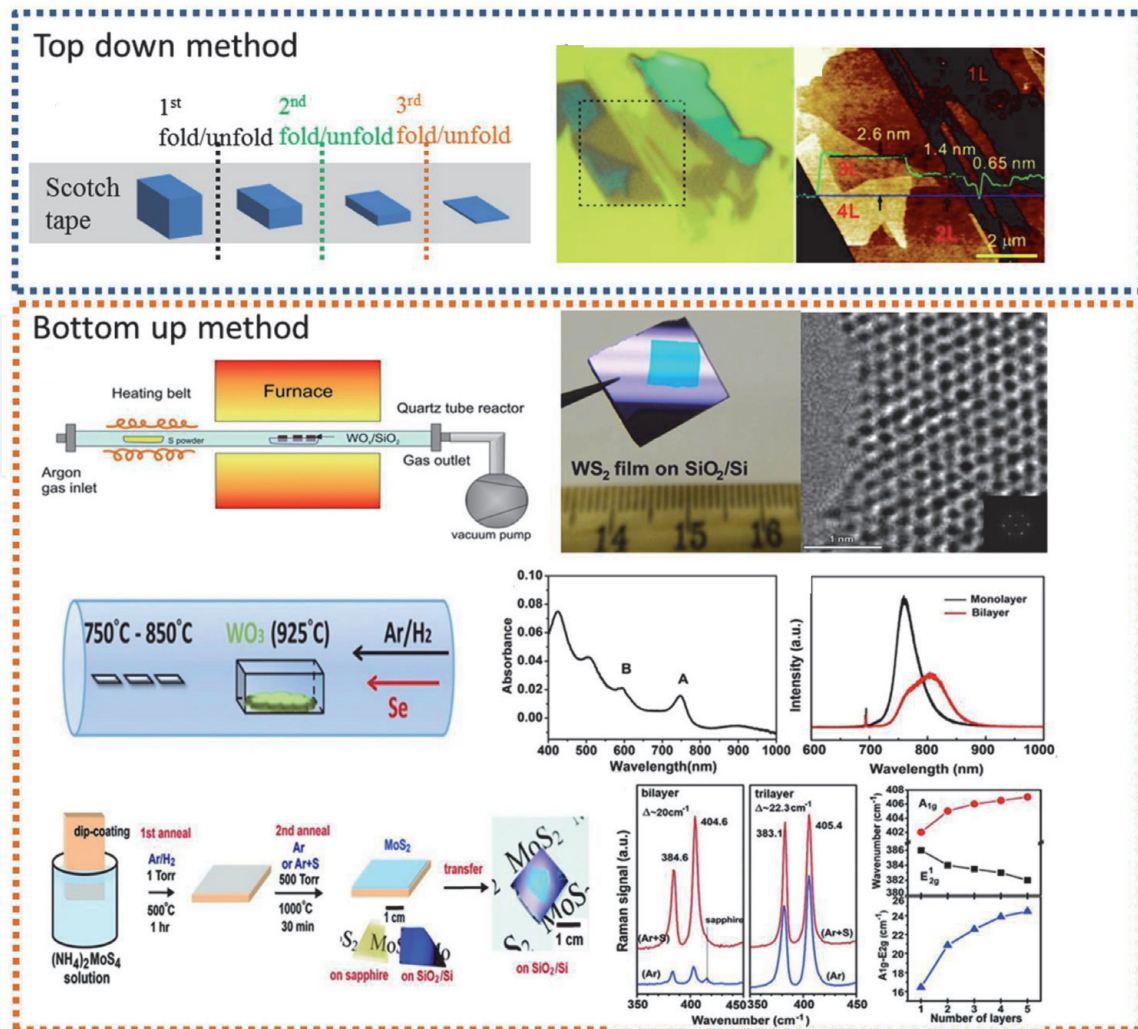
Figure 2.
Two routes of the TMC layer preparation: (top) a schematic representation of the top-down method – mechanical exfoliation and (bottom) a schematic illustration of the bottom-up method – CVD [22].

prepared from their bulk material by mechanical exfoliation are called the top-down method, while the TMC layers were produced from the elemental precursors on the target substrate in the bottom-up method, such as chemical vapor deposition (CVD) approach. The CVD method for TMC synthesis has been widely used due to its unique advantages such as scalable size, high crystallinity, and controllable thickness of TMCs [10–13]. One of the most classic TMCs, molybdenum sulfide (MoS_2), has been developed via CVD synthesis to replace the zero bandgap graphene. [14] There are two routes to synthesize MoS_2 layer by CVD (**Figure 3a**). One is a two-step growth route, where the Mo-based precursors are first deposited and then conducted the sulfurization or decomposition process to form MoS_2 (route 1, **Figure 3a**). The other growth way of MoS_2 layer is an one-step growth, where the gaseous Mo- and S-based precursors are simultaneously introduced and react to form MoS_2 on a substrate (route 2, **Figure 3a**). Recent reports have also demonstrated to grow MoS_2 on other kinds of insulating substrates such as quartz, mica, and sapphire (**Figure 3b**) [15, 16]. **Figure 3c** shows a typical experimental setup for the low-pressure CVD synthesis of MoS_2. The formation of entire MoS_2 would be prevented according to the ternary Mo—O—S phase diagram (**Figure 3d**) if the reducing atmosphere is too weak [17]. **Figure 3e** displays two possible mechanisms for the growth of MoS_2. The well-established CVD synthesis of MoS_2 is regarded as a prototype for the synthesis of other TMCs such as $MoSe_2$ and WS_2 [18, 19]. Except from the VI B group metals such as molybdenum and tungsten, the research works

of TMCs based on VIII B group metals such as cobalt [20] and nickel [21] are also widely studied in recent years.

2.2 Solvothermal synthesis of TMCs

Wet chemical synthesis, a bottom-up process, is broadly used to synthesize TMC nanosheets with tunable thickness and size [24–26]. The desired nanosheets form directly in solution or onto substrate in high yield. The synthesis of TMCs via wet chemical method usually relies on the chemical reaction of metal salts and sulfur/selenide-based materials as precursors. The solvothermal method is one of the most typical routes of wet chemical method, in which the reaction is conducted in a sealed autoclave at suitable temperature (**Figure 4**) [27]. As a representative example, Xie et al. [28] synthesized oxygen incorporated MoS_2 nanosheets from the
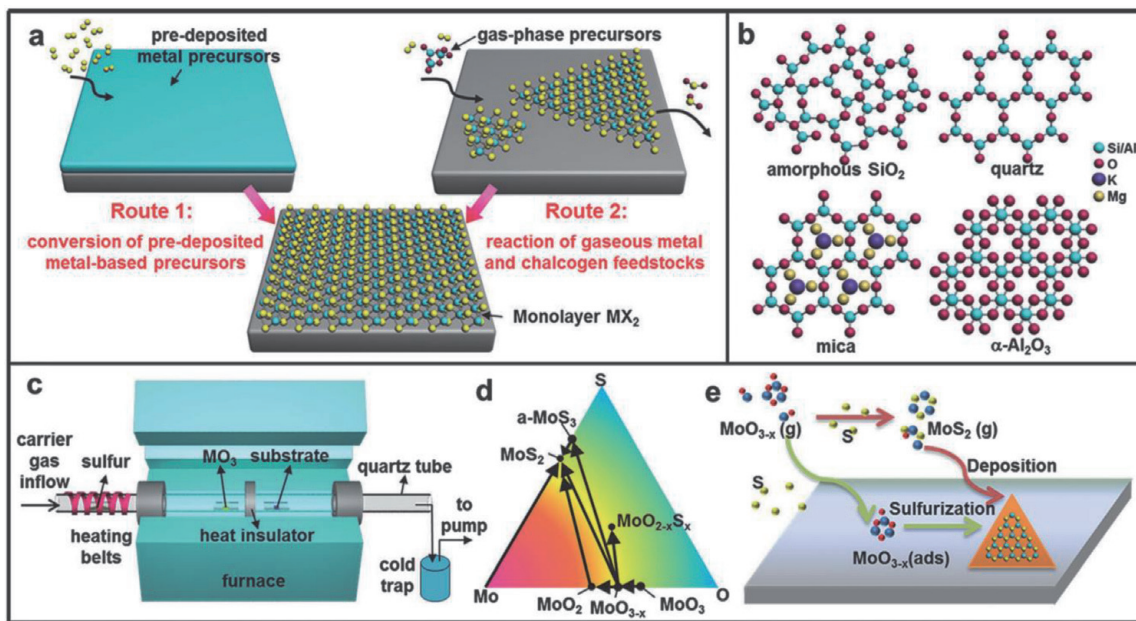

Figure 3.
The general introduction to the CVD synthesis, CVD setup, and growth mechanism of MoS₂ layer [23].
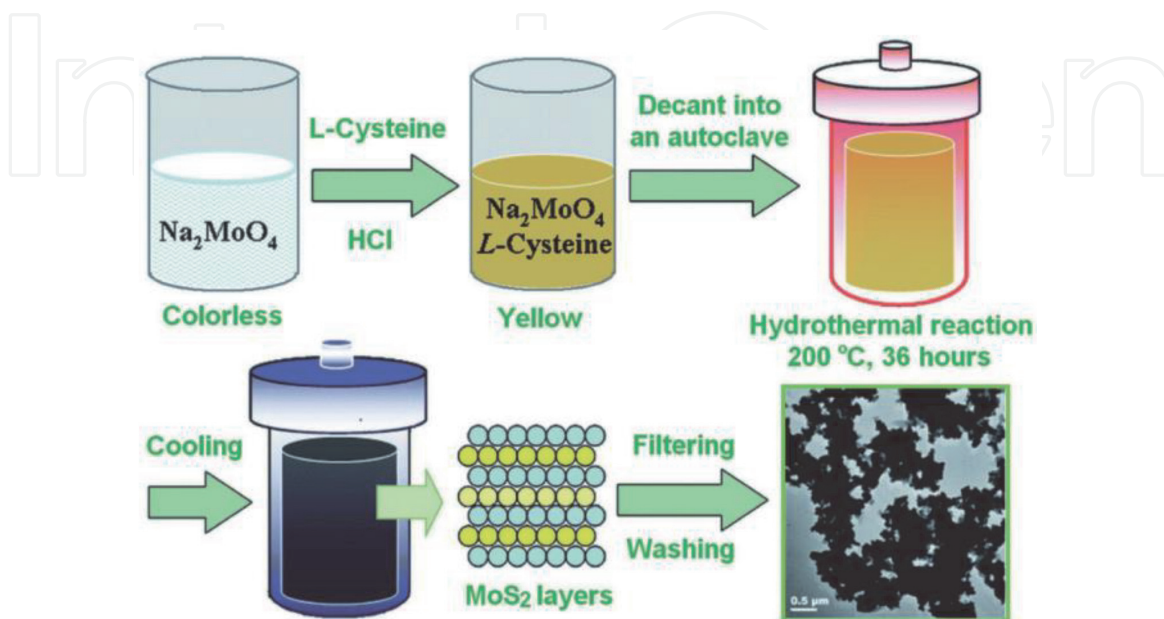

Figure 4.
The synthesis process of MoS₂ nanosheets via a simple hydrothermal method [27].
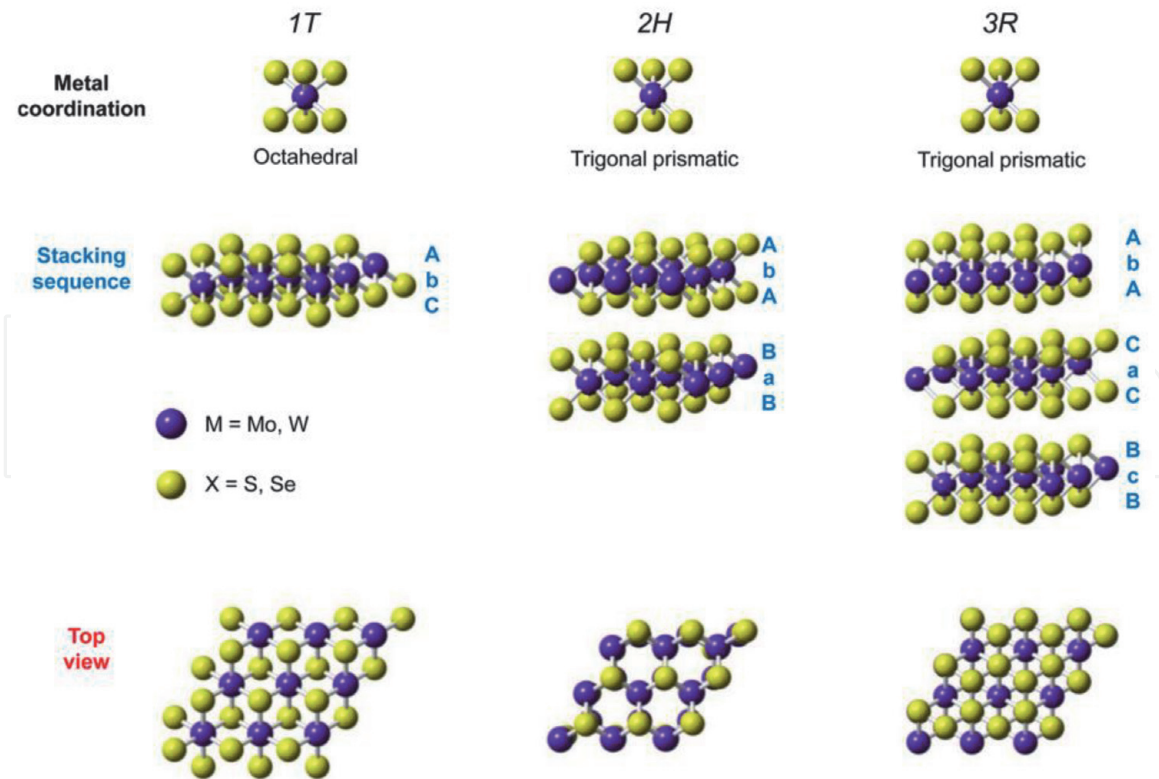
Figure 5.
Different metal coordination and stacking sequence in TMC unit cells [10].

precursors of $(NH_4)_6Mo_7O_{24}\cdot4H_2O$ and thiourea through a solvothermal method. By tuning the synthetic temperatures, the disordered structure and intrinsic conductivity of MoS_2 could be controlled to a moderate degree. Thus, the optimal catalyst for electrocatalytic hydrogen evolution reaction exhibits onset overpotential as low as 120 mV. It is well known that the materials with different crystal orientations have the anisotropic properties. This phenomenon appears in TMCs depending on stacking sequence of the chalcogen and transition-metal coordination. The commonly found polymorphs in TMC materials are the so-defined 1 T, 2H, and 3R, where the number and letter, respectively, indicate the layer number in the unit cell and the type of symmetry with T, H, and R representing for tetragonal, hexagonal, and rhombohedral, respectively (**Figure 5**). For example, Zhang et al. synthesized metallic CoS_2 nanopyramid array on carbon fiber paper by an one-step solvothermal synthesis [29]. In brief, the carbon fiber papers were transferred to the precursor solution containing $CoCl_2\cdot6H_2O$ and $CS(NH_2)_2$, which was maintained at 180°C for 12 hours. The unique 3D nanostructure and intrinsic metallic properties of the CoS_2 by this method contribute to the ultrahigh activity toward hydrogen evolution reaction.

3. Hydrogen evolution reaction (HER) based on TMC electrodes

In order to improve HER performance, three main factors including the number of active sites, intrinsic catalytic activity, and the conductivity of TMCs play crucial roles. In 2005, Hinnemann et al. suggested the active sites for HER only exist in the edges of TMCs by density functional theory (DFT) calculation [30]. Thus, many research works are dedicated to enrich the defect sites and/or active sites by nanostructural engineering [31–33]. Zhang et al. synthesized the edge-rich 3D MoS_2 coupling with conductive polymer polyaniline (PANI) as catalyst (**Figure 6**) [34].

The MoS$_2$ grown on 3D PANI substrate tends to grow vertically and expose abundant edge sites for HER. Consequently, excellent HER performance can be achieved with a low onset potential of 100 mV and a small Tafel slop of 45 mV dec^{-1}.
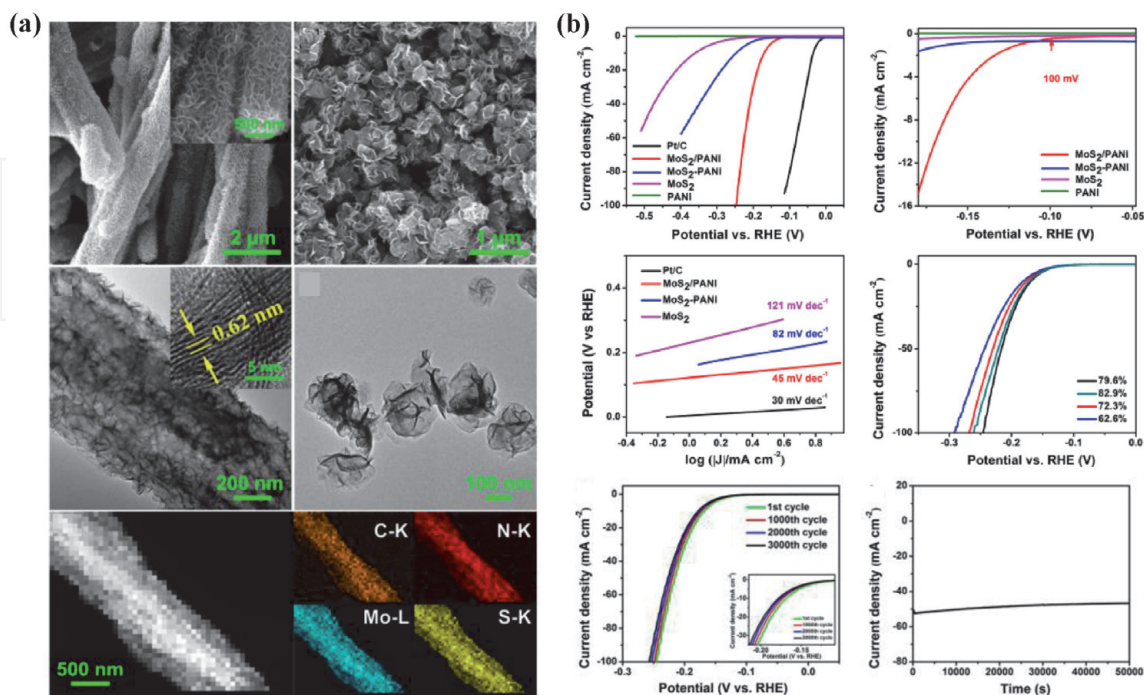

Figure 6.
The defect-rich 3D MoS$_2$/PANI catalyst for HER (a) the morphologies of synthesized 3D MoS$_2$/PANI and (b) the electrochemical performance of 3D MoS$_2$/PANI catalyst [34].
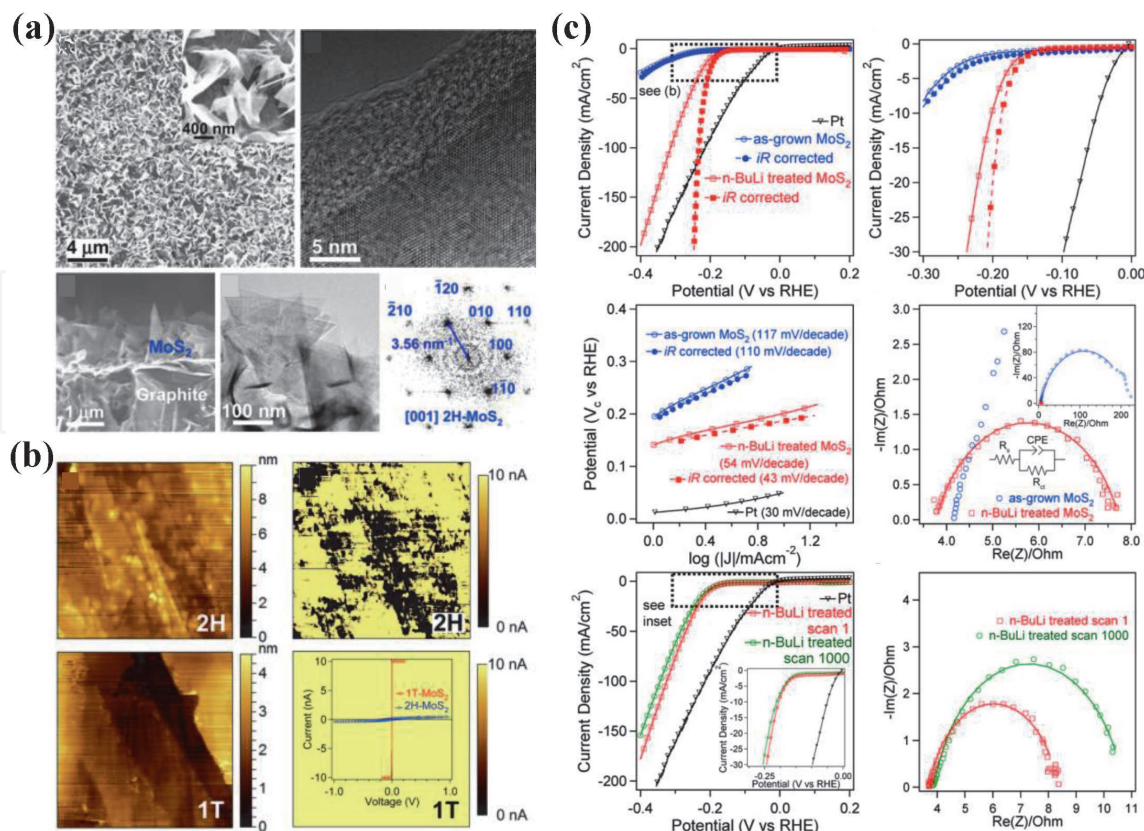

Figure 7.
(a) Electron microscopy characterization of as-grown 2H-MoS$_2$ nanostructures. (b) Comparison of as-grown and exfoliated MoS$_2$ nanosheets. (c) Electrocatalytic performance of chemically exfoliated and as-grown MoS$_2$ nanosheets [36].

Additionally, MoS_2/PANI achieved superior stability for HER electrocatalysis. Although the promising catalytic activity of MoS_2 for HER was achieved by creating abundant edge sites and/or active sites, the performance was still limited by its intrinsic properties such as poor electrical transport and inefficient electrical contact to the catalyst [35]. Lukowski et al. reported that the metallic nanosheets of 1T-MoS_2, which were chemically exfoliated by lithium intercalation of semiconducting 2H-MoS_2 nanostructures, dramatically enhanced HER performance (**Figure 7**) [36]. The current density of 10 mA cm^{-1} can be reached at a low overpotential of -187 mV with a Tafel slope of 43 mV dec^{-1}. The excellent performance can be attributed to the favorable kinetics, metallic conductivity, and increasing number of active sites in the metallic 1T-MoS_2 nanosheets, which was proven by the dramatically decrease of charge-transfer resistance from 232 Ω of 2H-MoS_2 nanostructures to 4 Ω of metallic 1T-MoS_2 nanosheets. This finding proves that the metallic 1T polymorph of TMCs is competitive to earth-abundant catalysts in heterogeneous catalysis.
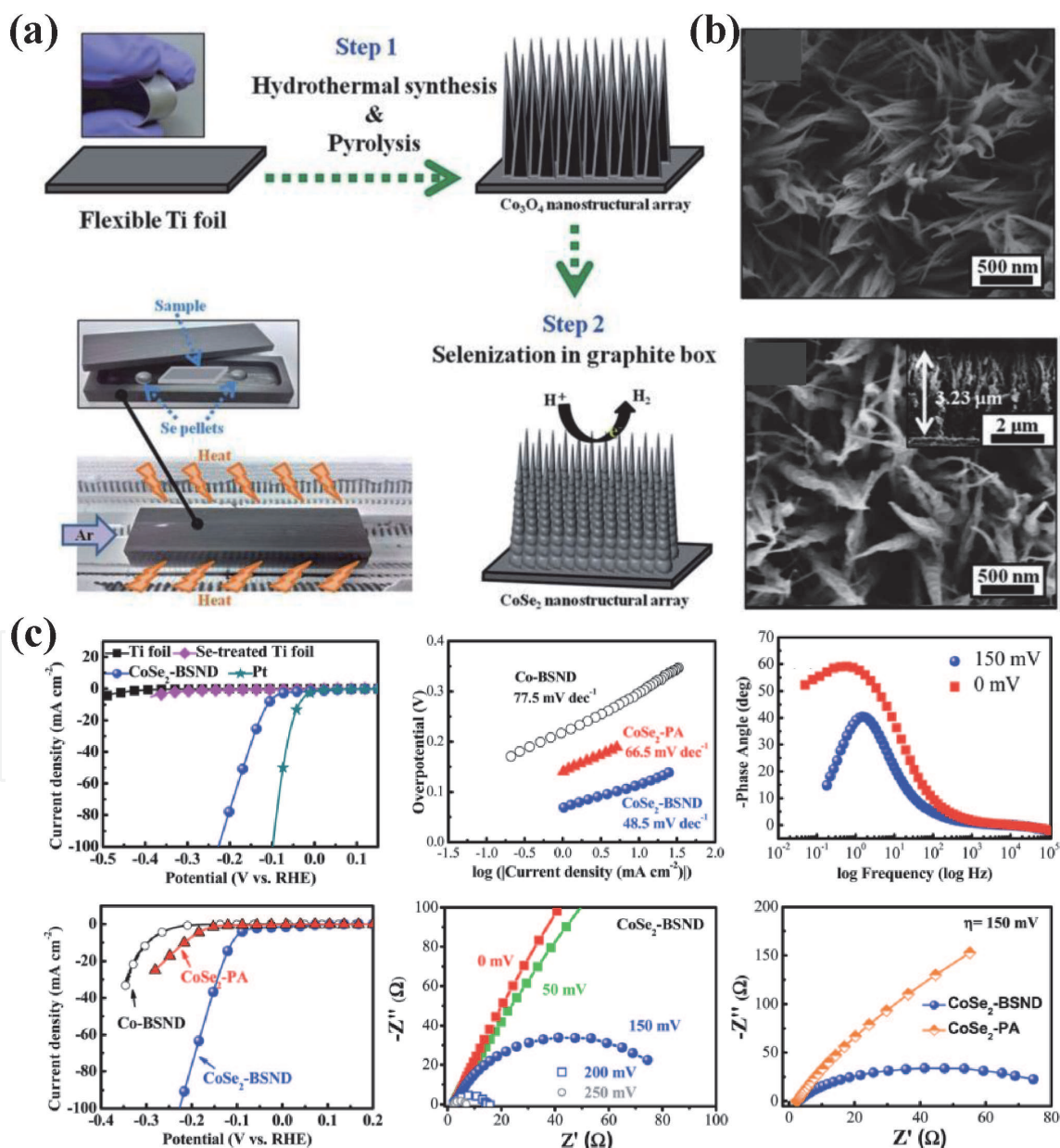

Figure 8.
(a) The schematic illustration for the synthesis of beaded stream-like $CoSe_2$ nanoneedles, (b) the SEM images of beaded stream-like ($CoSe_2$) nanoneedle array, and (c) the electrochemical measurements of Co-BSND, $CoSe_2$-PA, and $CoSe_2$-BSND electrodes [37].

Lee et al. developed earth-abundant nanostructuring beaded stream-like cobalt diselenide ($CoSe_2$) nanoneedles ($CoSe_2$-BSND) as electrocatalyst for HER [37]. The $CoSe_2$ nanoneedles derived from the cobalt oxide (Co_3O_4) nanoneedle array directly formed on flexible titanium foils after selenization treatment (**Figure 8**). The $CoSe_2$-BSND can drive the HER at a current density of 20 mA cm^{-2} with a small overpotential of 125 mV. Also, it possesses a small Tafel slope of 48.5 mV dec^{-1} suggesting that the HER follows the Volmer-Heyrovsky mechanism where a fast discharge of protons is followed by rate-determining electrochemical desorption. Moreover, the $CoSe_2$-BSND electrode achieved great stability in an acidic electrolyte for 3000 cycles. The enhanced electrochemical activity is attributed to the highly accessible surface active sites, the improved charge transfer kinetics, and the super hydrophilic surface of $CoSe_2$-BSND electrode.

4. Oxygen evolution reaction (OER) based on TMC electrodes

The TMC materials have shown promising performance toward HER as we mentioned above. Researchers are searching for the possibility of bifunctional electrocatalysts for both HER and OER to perform the overall water-splitting reaction. Moreover, TMC electrocatalysts have attracted tremendous attentions since Alonso-vante and coworker discovered that $Mo_4Ru_2Se_8$ had a ORR activity comparable to platinum [38]. As compared to ruthenium (Ru) and Rhenium (Rh), the low cost and earth abundant transition metals such as iron-, nickel- and cobalt-based TMCs have much attention for OER [39–41]. Liu and coworkers discovered that electrodeposited CoS nanosheet films on Ti mesh show high activity toward OER (**Figure 9**) [42]. The CoS nanosheets tend to drive a current density of 10 mA cm^{-2} with an overpotential of 361 mV. In addition, this electrode maintains highly catalytic activity for at least 20 hours. The superior catalytic activity along with excellent stability of CoS nanosheets offers the good opportunity to become a cost-effective and industry-feasible electrode toward OER. On the other hand, Swesi et al. first reported that the catalytic activity of OER was observed by the nickel selenide (Ni_3Se_2) in alkaline condition (**Figure 10**) [43]. The low overpotential
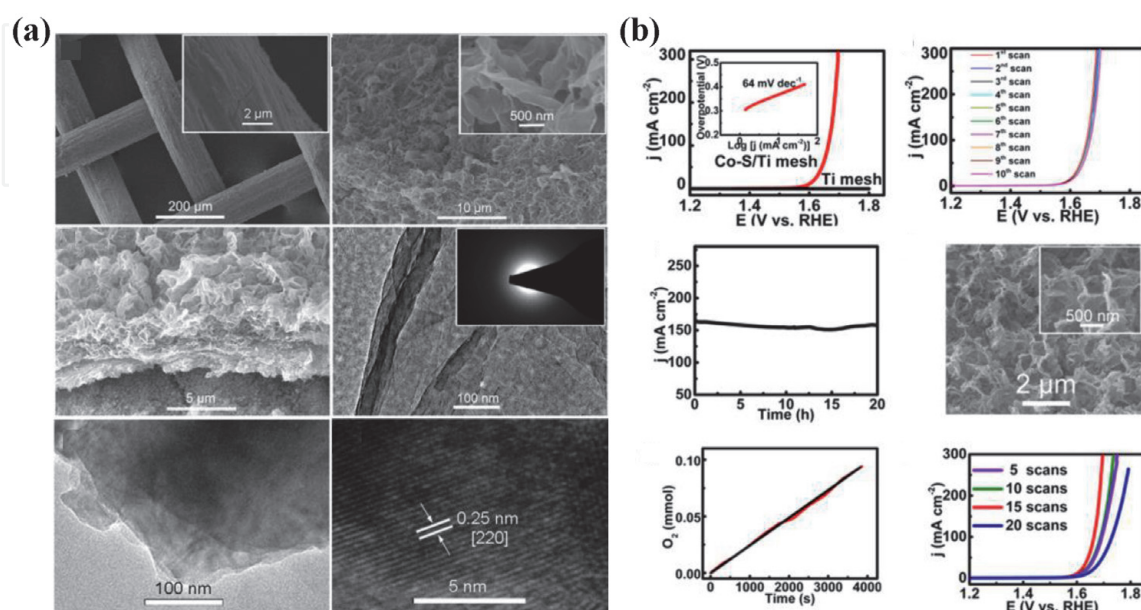

Figure 9.
(a) The surface morphology and crystal structure of electrodeposited CoS nanosheets and (b) the electrochemical performance and stability toward OER on CoS nanosheets [42].

required to reach 10 mA cm^{-2} was 290 mV, suggesting that this catalyst exhibits its competitivity among the oxide-based electrocatalysts. The catalytic ability of Ni$_3$Se$_2$ can be further improved through the modification of Se-deficient phase in Ni$_3$Se$_2$. Moreover, electrodeposited Ni$_3$Se$_2$ catalysts exhibited exceptional stability under OER for 42 hours. The effect of the underlying substrates such as glassy carbon, ITO-coated glass, and Ni foam on OER was also investigated. The results revealed that the glassy carbon substrate exhibited the lowest onset potential and the highest
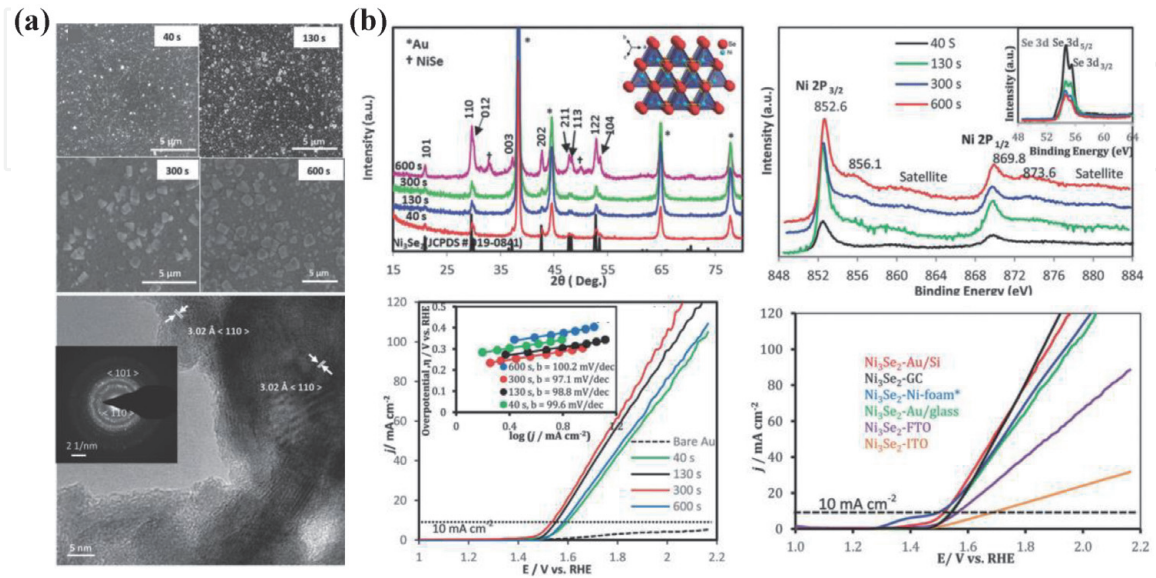

Figure 10.
(a) The morphological characterization of Ni$_3$Se$_2$ grown by electrochemical deposition and (b) the crystal structure identification and OER performance of Ni$_3$Se$_2$ electrocatalyst [43].
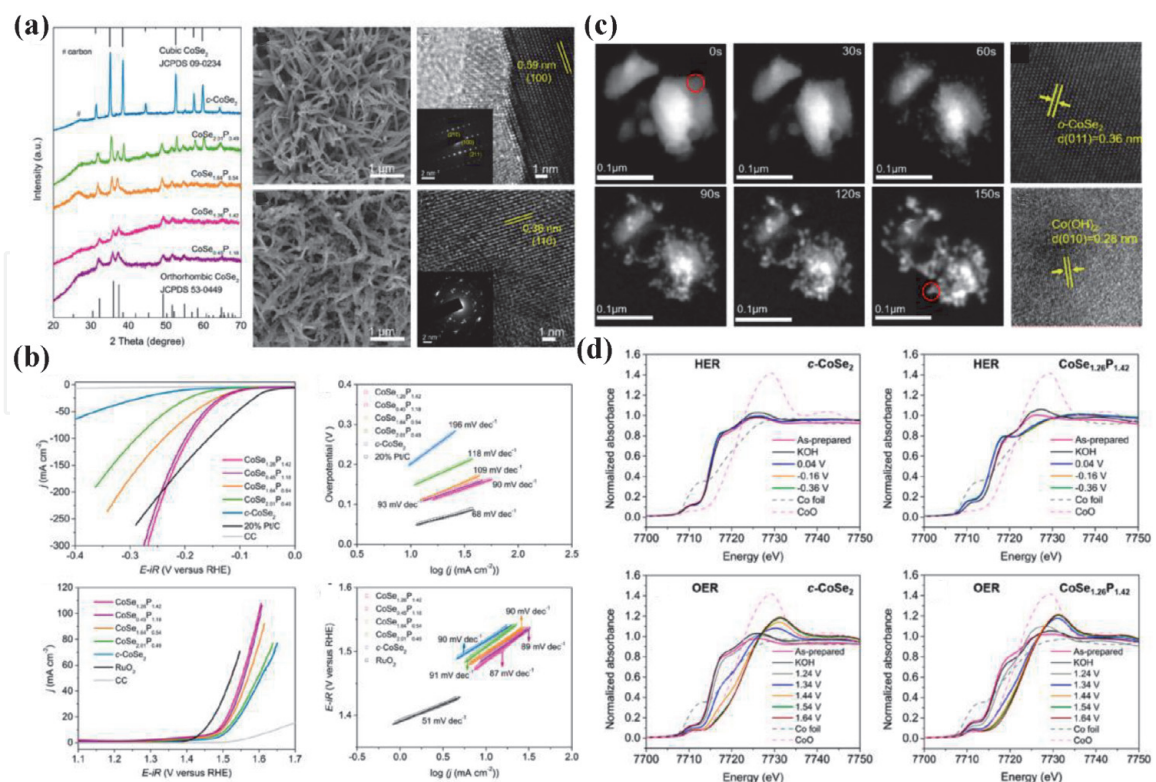

Figure 11.
(a) The structural and morphological characterizations of different P-doped CoSe$_2$, (b) electrochemical OER activities of the different P-doped CoSe$_2$ and standard RuO$_2$ electrodes, (c) in situ STEM images of the P-doped CoSe$_2$ catalyst taken at different times after immersing in the KOH solution, and (d) in situ Co K-edge XANES spectra of different P-doped CoSe$_2$ electrodes for HER and OER processes [3].

current density, suggesting that the interaction between the underlying substrate and the Ni_3Se_2 may play a role in O_2 evolution reaction.

Although the electrocatalytic performance of TMCs toward OER was significantly enhanced, the reaction mechanism and actual active sites responsible for the reaction were in dispute. Recently, operando or *in situ* experiments like *in situ* Fourier transform infrared spectroscopy, *in situ* Raman spectroscopy, and *in situ* X-ray absorption/diffraction are commonly carried out to provide atomic-level information [3, 44, 45]. Zhu and coworkers [3] conducted *in situ* X-ray absorption spectroscopy, *in situ* liquid-phase TEM, and *in situ* Raman spectroscopy, revealing that P-doped $CoSe_2$ in an alkaline solution was acting as the "pre-catalyst" rather than the real reactive species, which has been debated for a while (**Figure 11**). They found that the introduction of phosphorus would generate more vacancies, which facilitated the structural transformation into the real active electrocatalyst, such as metallic cobalt for HER and cobalt oxyhydroxide (CoOOH) for OER. $CoSe_{1.26}P_{1.42}$ shows the best OER performance among all catalysts, which requires an overpotential of 255 mV to reach the current density of 10 mA cm^{-2}. Furthermore, the $CoSe_{1.26}P_{1.42}$ catalyst with a Tafel slop of 87 mV dec^{-1} exhibits a slightly lower than those of the other P-doped $CoSe_2$ catalysts. Such performance is comparable to many leading earth-abundant HER and OER catalysts in alkaline electrolyte.

5. Conclusion

Electrocatalysts for HER and OER play an important role for sustainable energy, which require converting renewable energy to storable chemical fuels or employing clean energy. In this article, we have partially reviewed the promising candidates, transition metal (di)chalcogenides (TMCs), from preparation methods to electrochemical measurements toward HER and OER. It can be concluded that a good electrocatalyst should possess good conductivity and moderate adsorption energy to reactive species and/or intermediates. In addition, the large number of active/defect sites would be favorable for catalytic ability. The future challenges for TMCs toward HER and OER are summarized as follows. The realization of the mechanisms toward the HER and OER plays a key role to design a perfect electrocatalyst. The development of *in situ* or operando techniques shines the light on this difficulty. Most importantly, the understanding of HER and OER mechanisms offers the significant information to many other fields due to the similar operating concepts in electrocatalytic and photocatalytic applications.

Acknowledgements

Author details

Chi-Ang Tseng[1] and Chuan-Pei Lee[2]*

1 Department of Chemistry, National Taiwan University, Taiwan

2 Department of Applied Physics and Chemistry, University of Taipei, Taiwan

*Address all correspondence to: cplee@utaipei.edu.tw

IntechOpen

References

[1] Bockris JOM. The origin of ideas on a hydrogen economy and its solution to the decay of the environment. International Journal of Hydrogen Energy. 2002;**27**:731-740. DOI: 10.1016/S0360-3199(01)00154-9

[2] Dresselhaus MS, Thomas IL. Alternative energy technologies. Nature. 2001;**414**:332-337. DOI: 10.1038/35104599

[3] Zhu Y, Chen HC, Hsu CS, Lin TS, Chang CJ, Chang SC, et al. Operando unraveling of the structural and chemical stability of P-substituted $CoSe_2$ electrocatalysts toward hydrogen and oxygen evolution reactions in alkaline electrolyte. ACS Energy Letters. 2019;**4**:987-994. DOI: 10.1021/acsenergylett.9b00382

[4] Zhang J, Zhao Z, Xia Z, Dai L. A metal-free bifunctional electrocatalyst for oxygen reduction and oxygen evolution reactions. Nature Nanotechnology. 2015;**10**:444-452. DOI: 10.1038/nnano.2015.48

[5] Li Y, Wang H, Xie L, Liang Y, Hong G, Dai H. MoS_2 nanoparticles grown on graphene: An advanced catalyst for the hydrogen evolution reaction. Journal of the American Chemical Society. 2011;**133**:7296-7299. DOI: 10.1021/ja201269b

[6] Conway BE, Tilak BV. Interfacial processes involving electrocatalytic evolution and oxidation of H_2, and the role of chemisorbed H. Electrochimica Acta. 2002;**47**:3571-3594. DOI: 10.1016/S0013-4686(02)00329-8

[7] Zeng M, Li Y. Recent advances in heterogeneous electrocatalysts for the hydrogen evolution reaction. Journal of Materials Chemistry A. 2015;**3**:14942-14962. DOI: 10.1039/c5ta02974k

[8] Nørskov JK, Bligaard T, Logadottir A, Kitchin JR, Chen JG, Pandelov S, et al. Trends in the exchange current for hydrogen evolution. Journal of the Electrochemical Society. 2005;**152**:J23. DOI: 10.1149/1.1856988

[9] Suen NT, Hung SF, Quan Q, Zhang N, Xu YJ, Chen HM. Electrocatalysis for the oxygen evolution reaction: Recent development and future perspectives. Chemical Society Reviews. 2017;**46**:337-365. DOI: 10.1039/c6cs00328a

[10] Chia X, Eng AYS, Ambrosi A, Tan SM, Pumera M. Electrochemistry of nanostructured layered transition-metal dichalcogenides. Chemical Reviews. 2015;**115**:11941-11966. DOI: 10.1021/acs.chemrev.5b00287

[11] Huang JK, Pu J, Hsu CL, Chiu MH, Juang ZY, Chang YH, et al. Large-area synthesis of highly crystalline WSe_2 monolayers and device applications. ACS Nano. 2014;**8**:923-930. DOI: 10.1021/nn405719x

[12] Liu G, Li Z, Hasan T, Chen X, Zheng W, Feng W, et al. Vertically aligned two-dimensional SnS_2 nanosheets with a strong photon capturing capability for efficient photoelectrochemical water splitting. Journal of Materials Chemistry A. 2017;**5**:1989-1995. DOI: 10.1039/c6ta08327g

[13] Chang YH, Zhang W, Zhu Y, Han Y, Pu J, Chang JK, et al. Monolayer $MoSe_2$ grown by chemical vapor deposition for fast photodetection. ACS Nano. 2014;**8**:8582-8590. DOI: 10.1021/nn503287m

[14] Lee YH, Zhang XQ, Zhang W, Chang MT, TeLin C, DiChang K, et al. Synthesis of large-area MoS_2 atomic layers with chemical vapor deposition. Advanced Materials. 2012;**24**:2320-2325. DOI: 10.1002/adma.201104798

[15] Ji Q, Zhang Y, Gao T, Zhang Y, Ma D, Liu M, et al. Epitaxial monolayer

MoS_2 on mica with novel photoluminescence. Nano Letters. 2013;**13**:3870-3877. DOI: 10.1021/nl401938t

[16] Yu Y, Li C, Liu Y, Su L, Zhang Y, Cao L. Controlled scalable synthesis of uniform, high-quality monolayer and few-layer MoS_2 films. Scientific Reports. 2013;**3**:1-6. DOI: 10.1038/srep01866

[17] Feldman Y, Tenne R, Wasserman E, Srolovitz DJ. High-rate, gas-phase growth of MoS_2 nested inorganic fullerenes and nanotubes. Science. 1995; **267**:222

[18] Zhao Y, Lee H, Choi W, Fei W, Lee CJ. Large-area synthesis of monolayer $MoSe_2$ films on SiO_2/Si substrates by atmospheric pressure chemical vapor deposition. RSC Advances. 2017;**7**:27969-27973. DOI: 10.1039/c7ra03642f

[19] Okada M, Sawazaki T, Watanabe K, Taniguch T, Hibino H, Shinohara H, et al. Direct chemical vapor deposition growth of WS_2 atomic layers on hexagonal boron nitride. ACS Nano. 2014;**8**:8273-8277. DOI: 10.1021/nn503093k

[20] Wang B, Wang Z, Wang X, Zheng B, Zhang W, Chen Y. Scalable synthesis of porous hollow $CoSe_2$-$MoSe_2$/carbon microspheres for highly efficient hydrogen evolution reaction in acidic and alkaline media. Journal of Materials Chemistry A. 2018;**6**: 12701-12707. DOI: 10.1039/c8ta03523g

[21] An T, Wang Y, Tang J, Wei W, Cui X, Alenizi AM, et al. Interlaced NiS_2-MoS_2 nanoflake-nanowires as efficient hydrogen evolution electrocatalysts in basic solutions. Journal of Materials Chemistry A. 2016; **4**:13439-13443. DOI: 10.1039/c6ta05022k

[22] Dong R, Kuljanishvili I. Review article: Progress in fabrication of transition metal dichalcogenides heterostructure systems. Journal of Vacuum Science and Technology B. 2017;**35**:030803. DOI: 10.1116/1.4982736

[23] Ji Q, Zheng Y, Zhang Y, Liu Z. Chemical vapour deposition of group-VIB metal dichalcogenide monolayers: Engineered substrates from amorphous to single crystalline. Chemical Society Reviews. 2015;**44**:2587-2602. DOI: 10.1039/c4cs00258j

[24] Wang S, Chen Y, Li X, Gao W, Zhang L, Liu J, et al. Injectable 2D MoS_2-integrated drug delivering implant for highly efficient NIR-triggered synergistic tumor hyperthermia. Advanced Materials. 2015;**27**:7117-7122. DOI: 10.1002/adma.201503869

[25] Cheng L, Yuan C, Shen S, Yi X, Gong H, Yang K, et al. Bottom-up synthesis of metal-ion-doped WS_2 nanoflakes for cancer theranostics. ACS Nano. 2015;**9**:11090-11101. DOI: 10.1021/acsnano.5b04606

[26] Shen S, Chao Y, Dong Z, Wang G, Yi X, Song G, et al. Bottom-up preparation of uniform ultrathin rhenium disulfide nanosheets for image-guided photothermal radiotherapy. Advanced Functional Materials. 2017;**27**: 1-9. DOI: 10.1002/adfm.201700250

[27] Zhu S, Gong L, Xie J, Gu Z, Zhao Y. Design, synthesis, and surface modification of materials based on transition-metal dichalcogenides for biomedical applications. Small Methods. 2017;**1**:1700220. DOI: 10.1002/smtd.201700220

[28] Xie J, Zhang J, Li S, Grote F, Zhang X, Zhang H, et al. Controllable disorder engineering in oxygen-incorporated MoS_2 ultrathin nanosheets for efficient hydrogen evolution. Journal of the American Chemical Society. 2013; **135**:17881-17888. DOI: 10.1021/ja408329q

[29] Zhang H, Li Y, Zhang G, Xu T, Wan P, Sun X. A metallic CoS_2 nanopyramid array grown on 3D carbon

fiber paper as an excellent electrocatalyst for hydrogen evolution. Journal of Materials Chemistry A. 2015; **3**:6306-6310. DOI: 10.1039/c5ta00707k

[30] Hinnemann B, Moses PG, Bonde J, Jørgensen KP, Nielsen JH, Horch S, et al. Biomimetic hydrogen evolution: MoS$_2$ nanoparticles as catalyst for hydrogen evolution. Journal of the American Chemical Society. 2005;**127**:5308-5309. DOI: 10.1021/ja0504690

[31] Ren X, Pang L, Zhang Y, Ren X, Fan H, Liu S. One-step hydrothermal synthesis of monolayer MoS$_2$ quantum dots for highly efficient electrocatalytic hydrogen evolution. Journal of Materials Chemistry A. 2015;**3**:10693-10697. DOI: 10.1039/c5ta02198g

[32] Du H, Gu S, Liu R, Li CM. Tungsten diphosphide nanorods as an efficient catalyst for electrochemical hydrogen evolution. Journal of Power Sources. 2015;**278**:540-545. DOI: 10.1016/j.jpowsour.2014.12.095

[33] Zhang X, Li L, Guo Y, Liu D, You T. Amorphous flower-like molybdenum-sulfide-at-nitrogen-doped-carbon-nanofiber film for use in the hydrogen-evolution reaction. Journal of Colloid and Interface Science. 2016;**472**:69-75. DOI: 10.1016/j.jcis.2016.03.041

[34] Zhang N, Ma W, Wu T, Wang H, Han D, Niu L. Edge-rich MoS$_2$ naonosheets rooting into polyaniline nanofibers as effective catalyst for electrochemical hydrogen evolution. Electrochimica Acta. 2015;**180**:155-163. DOI: 10.1016/j.electacta.2015.08.108

[35] Laursen AB, Kegnæs S, Dahl S, Chorkendorff I. Molybdenum sulfides-efficient and viable materials for electro- and photoelectrocatalytic hydrogen evolution. Energy & Environmental Science. 2012;**5**:5577-5591. DOI: 10.1039/c2ee02618j

[36] Lukowski MA, Daniel AS, Meng F, Forticaux A, Li L, Jin S. Enhanced hydrogen evolution catalysis from chemically exfoliated metallic MoS$_2$ nanosheets. Journal of the American Chemical Society. 2013;**135**:10274-10277. DOI: 10.1021/ja404523s

[37] Lee CP, Chen WF, Billo T, Lin YG, Fu FY, Samireddi S, et al. Beaded stream-like CoSe$_2$ nanoneedle array for efficient hydrogen evolution electrocatalysis. Journal of Materials Chemistry A. 2016;**4**:4553-4561. DOI: 10.1039/c6ta00464d

[38] Vante NA, Tributsch H. Energy conversion catalysis using semiconducting transition metal cluster compounds. Nature. 1986;**323**:431-432

[39] Feng Y, He T, Alonso-vante N. In situ free-surfactant synthesis and ORR-electrochemistry of carbon-supported Co$_3$S$_4$ and CoSe$_2$ nanoparticles. Chemistry of Materials. 2008;**20**:26-28

[40] Gao MR, Jiang J, Yu SH. Solution-based synthesis and design of late transition metal chalcogenide materials for oxygen reduction reaction (ORR). Small. 2012;**8**:13-27. DOI: 10.1002/smll.201101573

[41] Gao MR, Xu YF, Jiang J, Yu SH. Nanostructured metal chalcogenides: Synthesis, modification, and applications in energy conversion and storage devices. Chemical Society Reviews. 2013;**42**:2986-3017. DOI: 10.1039/c2cs35310e

[42] Liu T, Liang Y, Liu Q, Sun X, He Y, Asiri AM. Electrodeposition of cobalt-sulfide nanosheets film as an efficient electrocatalyst for oxygen evolution reaction. Electrochemistry Communications. 2015;**60**:92-96. DOI: 10.1016/j.elecom.2015.08.011

[43] Swesi AT, Masud J, Nath M. Nickel selenide as a high-efficiency catalyst for oxygen evolution reaction. Energy & Environmental Science. 2016;**9**:1771-1782. DOI: 10.1039/C5EE02463C

[44] Deng Y, Handoko AD, Du Y, Xi S, Yeo BS. In situ Raman spectroscopy of copper and copper oxide surfaces during electrochemical oxygen evolution reaction: Identification of CuIII oxides as catalytically active species. ACS Catalysis. 2016;**6**: 2473-2481. DOI: 10.1021/ acscatal.6b00205

[45] Zhang M, DeRespinis M, Frei H. Time-resolved observations of water oxidation intermediates on a cobalt oxide nanoparticle catalyst. Nature Chemistry. 2014;**6**:362-367. DOI: 10.1038/nchem.1874